Received: 3 May 2022 | Revised: 4 August 2022 | Accepted: 10 September 2022

DOI: 10.1111/jeb.14115

JOURNAL OF Evolutionary Biology eseb

RESEARCH ARTICLE

Can extreme climatic events induce shifts in adaptive potential? A conceptual framework and empirical test with *Anolis* lizards

Monique N. Simon[1] | **Priscila S. Rothier**[2] | **Colin M. Donihue**[3] | **Anthony Herrel**[4,5,6] | **Jason J. Kolbe**[7]

[1]Department of Integrative Biology, Oklahoma State University, Stillwater, Oklahoma, USA

[2]UMR 7179, Muséum National d'Histoire Naturelle, Paris, France

[3]Institute at Brown for Environment and Society, Brown University, Providence, Rhode Island, USA

[4]UMR 7179, Centre National de la Recherche Scientifique/Muséum National d'Histoire Naturelle, Paris, France

[5]Functional Morphology Lab, Department of Biology, University of Antwerp, Wilrijk, Belgium

[6]Evolutionary Morphology of Vertebrates, Ghent University, Ghent, Belgium

[7]Department of Biological Sciences, University of Rhode Island, Kingston, Rhode Island, USA

Correspondence

Monique N. Simon, Department of Integrative Biology, Oklahoma State University, Stillwater OK, 74075, USA.
Email: monique.nouailhetas@gmail.com

Funding information

Pine Cay Homeowners Association; US National Science Foundation

Abstract

Multivariate adaptation to climatic shifts may be limited by trait integration that causes genetic variation to be low in the direction of selection. However, strong episodes of selection induced by extreme climatic pressures may facilitate future population-wide responses if selection reduces trait integration and increases adaptive potential (i.e., evolvability). We explain this counter-intuitive framework for extreme climatic events in which directional selection leads to increased evolvability and exemplify its use in a case study. We tested this hypothesis in two populations of the lizard *Anolis scriptus* that experienced hurricane-induced selection on limb traits. We surveyed populations immediately before and after the hurricane as well as the offspring of post-hurricane survivors, allowing us to estimate both selection and response to selection on key functional traits: forelimb length, hindlimb length, and toepad area. The direct selection was parallel in both islands and strong in several limb traits. Even though overall limb integration did not change after the hurricane, both populations showed a non-significant tendency toward increased evolvability after the hurricane despite the direction of selection not being aligned with the axis of most variance (i.e., body size). The population with comparably lower between-limb integration showed a less constrained response to selection. Hurricane-induced selection, not aligned with the pattern of high trait correlations, likely conflicts with selection occurring during normal ecological conditions that favours functional coordination between limb traits, and would likely need to be very strong and more persistent to elicit a greater change in trait integration and evolvability. Future tests of this hypothesis should use G-matrices in a variety of wild organisms experiencing selection due to extreme climatic events.

KEYWORDS

extreme climate, limb morphology, lizards, locomotion, natural selection

1 | INTRODUCTION

Despite the vast literature focusing on adaptation to climate, predictions for how species will respond to climate change generally ignore the degree of adaptive potential of populations in the face of these changes, especially when multiple traits are under selection (Nadeau & Urban, 2019; but see Etterson, 2004; Etterson & Shaw, 2001; Peschel et al., 2021). Adaptive responses to climatic pressures can alter the ecological responses of populations, lowering their vulnerability to future changes, or even rescuing populations from extinction (Diniz-Filho et al., 2019; Quintero & Wiens, 2013). Of course, these adaptive responses depend on standing genetic variation in the traits under selection, the frequency and severity of climatic perturbations that induce selection and even on interactions with other species (Grant et al., 2017). For instance, we may expect adaptation to be especially challenging in response to extreme climatic events that induce very strong episodes of selection, leading to high mortality and small population sizes that may never rebound. Given that extreme climatic events are likely to become more frequent and intense with future climate change, such as accelerating warming rate (Fischer et al., 2021), the potential of populations facing extreme events to adapt and persist may be limited. However, the scenario may not be so daunting if populations can increase their adaptive potential in response to predicted extreme climatic events.

In this paper, we lay out a conceptual framework for the intriguing possibility that directional selection may increase the adaptive potential of populations by reorganizing genetic variance such that it aligns more with the direction of selection (Pavlicev et al., 2011), such as when selection is caused by extreme climatic pressures. Then we show how to apply this framework with a case study of hurricane-induced selection on functional traits in *Anolis* lizards. Although our data set has some important limitations which we discuss, such as only phenotypic (and no genetic) data and limited sample sizes, our goal is to stimulate future research on evolvability and extreme climatic events, a theme that is currently underappreciated in the literature.

1.1 | Genetic integration, constraint and evolvability

Given that selection induced by climate is likely on several traits at once, an important determinant of population-level responses is phenotypic and genetic integration among traits (Etterson & Shaw, 2001). Theoretical models posit that if selection induced by changes in the climate acts on several traits (i.e., multivariate selection; Lande, 1979; Lande & Arnold, 1983) that are tightly integrated—showing high genetic correlations—the response to selection may deviate from the direction of selection (Chevin, 2012; Hellmann & Pineda-Krch, 2007). Genetic trait integration is measured by the additive genetic variance–covariance matrix, the G-matrix (*G*), which has trait variances along its diagonal and trait covariances in the off-diagonal and characterizes the pattern of trait co-inheritance (Arnold et al., 2008; Lande, 1979). The response to selection is then determined by an interaction between directional selection and the G-matrix: $\Delta z = G\beta$; in which Δz is the evolutionary response vector and β is the selection gradient, which measures only the direct selection on traits by accounting for phenotypic trait correlations (Cheverud, 1984; Lande & Arnold, 1983).

High genetic integration among traits results in a very stretched *G* that accumulates additive variance in only one or a few trait combinations (a 'cigar-shaped' G-matrix, in contrast with a 'ball-shaped' G-matrix; see Figure 1), whereas most trait combinations will have little additive genetic variance (Arnold et al., 2001; Walsh & Blows, 2009). Therefore, the shape of *G* (i.e., how genetic variance is distributed along trait combinations) is crucial for determining how much additive variation will be available in the direction of β, that is, how high is the evolvability or the ability of a population to adapt (Hansen & Houle, 2008; Houle, 1992). In highly integrated systems, if the direction of β is not aligned with the combinations of traits accumulating genetic variance, *G* will have low evolvability in the direction of β and Δz will deviate from the direction of selection (Arnold et al., 2001; scenario B in Figure 1). Thus, whether populations will respond adaptively to climate-induced selection depends on evolvability: the higher the evolvability, the more likely the response to selection will be effectively adaptive. However, populations may be able to escape low evolvability if selection induced by climate events can change the shape of *G* to become more aligned with the direction of selection (i.e., more additive genetic variance in the direction of selection; e.g., Assis et al., 2016).

1.2 | Rapid shifts in evolvability and strong selection induced by climatic extremes

Pavlicev et al. (2011) presented a theoretical model in which directional selection changes the pattern of trait integration (i.e., changing the shape of *G*), by acting on genes that regulate the degree of association between traits (the so-called 'rQTLs', relationship Quantitative Trait Loci; Cheverud et al., 2004; Pavlicev et al., 2008). The fundamental idea is that rQTLs change the effects of loci that control more than one trait (pleiotropic loci), which are one of the genetic bases for trait correlations together with linkage disequilibrium. Therefore, this model depends on genetic variation in pleiotropy, which was shown to be produced by interactions of pleiotropic loci with different rQTLs (i.e., differential epistasis; Pavlicev et al., 2008). Importantly, selection on rQTLs can change genetic variation without an appreciable effect on trait means (Cheverud et al., 2004; Pavlicev et al., 2008). Thus, different genotypes at rQTLs result in different G-matrices, and if they also show differences in mean fitness, selection will favour a specific *G* and may culminate in changes in the population covariance structure after several generations.

The most interesting result of this model is that *G* stretches in the direction of selection, that is, the combination of traits with the highest additive variance gets aligned with the direction of selection, increasing evolvability (Pavlicev et al., 2011). This happens

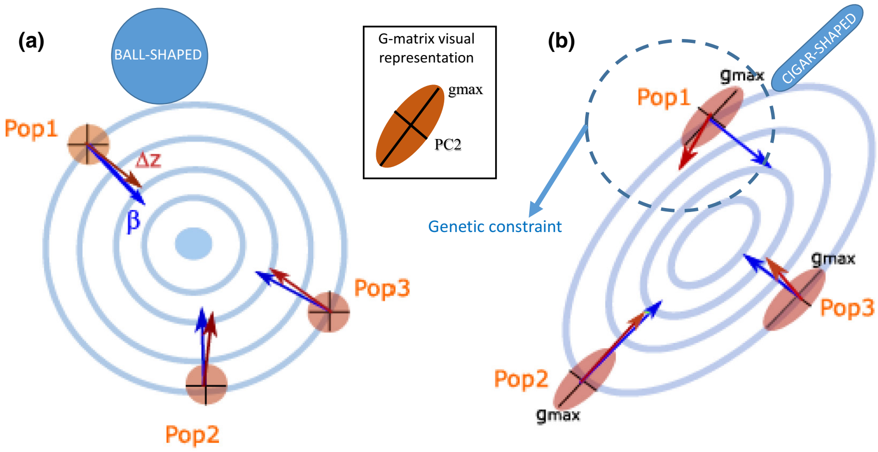

FIGURE 1 Visual representation of the G-matrix and its interaction with directional selection (β) to produce an evolutionary response (Δz). The G-matrix is generally represented by the directions of its first and second axes of variation (PC1 or gmax, and PC2, respectively). Selection is represented as a selection surface (or fitness landscape, blue contour lines) and the direction of selection as blue arrows. In scenario a, the G-matrix has low integration between traits, showing a *ball-shaped representation*. Because the genetic integration is low, the evolutionary response (red arrows) follows the direction of selection independent of the position of populations in relation to the selection surface. In scenario b, the G-matrix has high integration between traits, showing a *cigar-shaped representation*, with most variance accumulating in the direction of gmax. In this scenario, the evolutionary response may not follow the direction of selection, representing a case of genetic constraint, as shown for population 1 (Pop 1). However, if the selection is aligned with gmax (Pop 2) or with PC2 (Pop 3), the evolutionary response will follow the direction of selection even with high genetic integration between traits. Figure adapted from Arnold et al. (2001).

because the rQTL genotype with higher variance along the direction of selection has higher fitness. The change in *G* is gradual across generations until the most advantageous genotype is fixed by selection (Figure 2a). Hence, this model posits that directional selection can theoretically change genetic trait integration to increase heritable variation in the direction of selection. This is different from what is predicted with a more traditional view of selection acting strictly on additive variation without epistasis, which would result in no change in genetic variance, and therefore no change in evolvability after selection when considering polygenetic traits and mutation-selection equilibrium (i.e., the genetic variation that is removed by selection is replenished by mutation; Burger, 1993; Hill, 1982). However, both the model of Pavlicev et al. (2011) and evolutionary simulations of the mutational matrix (M-matrix; Jones et al., 2014; Melo & Marroig, 2015) indicate that gene interactions (epistasis) are a crucial factor to allow the alignment between the M-matrix, the G-matrix and directional selection. More importantly, an increase in evolvability can happen quite fast, only after 100 years of directional selection on chipmunks in natural conditions (Assis et al., 2016) and after 50 generations of artificial selection on mice (Penna et al., 2017).

If climate-induced selection elicits a change in *G* such that more additive variation accumulates in the direction of selection, populations may be more prone to evolve adaptively to the same climatic factor in the future, even if traits are strongly integrated before the action of selection. This scenario may be even more relevant for population survival in face of rapid climate change if selection induced by climatic events is strong. Extreme climatic events, which are historically rare but increasing in frequency, may induce strong episodes of directional selection (Grant et al., 2017). Such selection has the potential to change not only trait means but also change the pattern of trait integration, culminating in a shift in evolvability. It is important to note that the Pavlicev et al. (2011) simulations were done with very weak selection (selection coefficients of 0.001 or 0.05), and still the change in *G* could happen in less than 50 generations depending on the level of genetic linkage (Figure 2a,b). Yet, with very strong selection induced by extreme climatic pressures, a small change in *G* could happen very fast, perhaps in just a single generation, but being enough to increase evolvability in a biologically meaningful amount (Figure 2c).

We test this new hypothesis using lizard limb traits subjected to selection induced by hurricanes to demonstrate how this framework can be applied in future studies. Different from previous studies showing increased evolvability after selection (Assis et al., 2016; Pavlicev et al., 2008; Penna et al., 2017), we test this hypothesis on a system in which selection is not on the main axis of variation, which is body size here and in many other studies. It is unclear whether evolvability can increase with a directional selection that is not aligned with the axis of greatest variation. In this case study, we use P-matrices as surrogates of G-matrices, and our results suggest that extreme climatic events could lead to increased evolvability in some populations. However, we caution that the ultimate test needs to be performed with G-matrices and larger sample sizes. An analytical framework developed by Grabowski and Porto (2017) can be used to estimate the minimum sample sizes needed to find significant changes in evolvability. Nevertheless, we emphasize that having ideal samples to study unpredictable extreme events in nature is quite difficult, and thus, we must work with the available data to

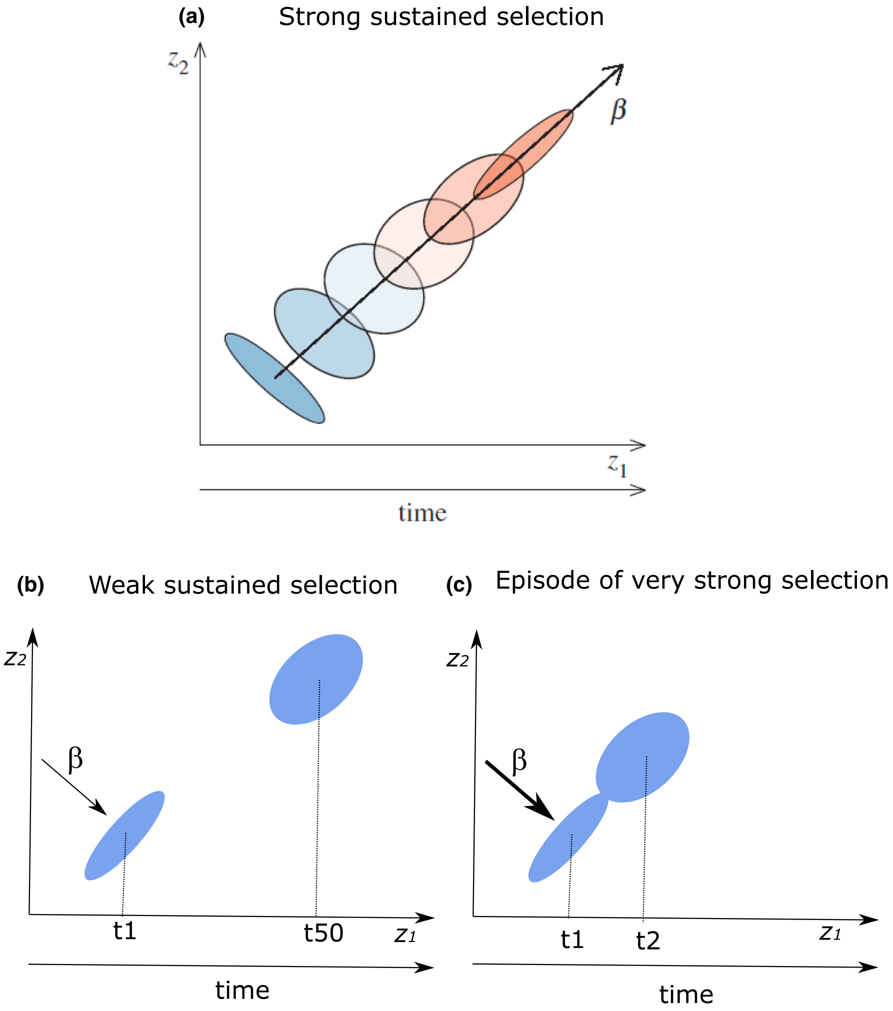

FIGURE 2 Conceptual framework of directional selection shifting evolvability. (a) a population under strong sustained selection gradually changes its G-matrix (elipse) to first become less integrated and then aligning completely with the direction of selection, leading to increased evolvability. Adapted from Assis et al. (2016). (b) under weak sustained selection, we expect the G-matrix to show lower integration only after some generations (50 generations in this example). (c) under very strong selection, such as the one induced by extreme climatic events, the G-matrix may show lower integration in just a single generation, also increasing evolvability in the direction of selection, despite not being completely aligned with the direction of selection.

reach an understanding of the potential impacts of these increasingly common phenomena on biodiversity.

1.3 | Case study: Hurricane-induced selection on lizard limb traits

We focused on two populations of the lizard *Anolis scriptus* that were exposed to Hurricanes Irma and Maria in 2017, showing strong selection of limb traits induced by this extreme climatic event (Donihue et al., 2018). In both populations, the toepad area became larger, relative humerus length became longer, whereas relative femur length was shorter in survivors of the hurricane. These morphological changes were shown to be associated with higher clinging capacity and reduced aerodynamic drag, performances that are likely relevant to increase survival in the face of hurricanes (Debaere et al., 2021; Donihue et al., 2018). These populations were re-surveyed in 2019 and data on the offspring of the survivors were collected, allowing for the assessment of the degree to which the evolutionary responses to selection in the offspring (Δz) followed the direction of selection (β). Toepad area is likely heritable because the offspring of survivors from the hurricane also had large toepads (Donihue et al., 2020). Although this change could be due to phenotypic plasticity, limb traits are moderately to highly heritable. Narrow-sense heritability of hindlimb has been measured in *Anolis sagrei*, exhibiting quite high values (0.78 ± 0.13, see Calsbeek & Bonneaud, 2008). Significant genetic variance in limb length was also measured in five species of *Anolis*, where heritabilities varied from 0.45 to 0.54 for the femur and tibia, and around 0.15 for humerus and ulna (McGlothlin et al., 2018). Therefore, the limb structures of *Anolis* that we are dealing with comprise heritable traits that show additive variance that can be moulded by selection.

Because we know that hurricane-induced selection is multivariate and limb traits are expected to be highly integrated in lizards, we need to analyse more than just a single trait for a robust understanding of the response to selection and whether evolvability changes after this episode of strong selection. Morphological integration of limb traits has been characterized in different *Anolis* species, showing that phenotypic correlations are generally high among limb elements (Kolbe et al., 2011). Recent studies in *Anolis* species revealed that genetic correlations are also high between limb traits (McGlothlin et al., 2018, 2021). High positive between-limb genetic correlations mean that it is easier to change all limb traits in the same direction (increasing or reducing all limb traits; directions that bear high genetic variation) than changing just fore- or hindlimb traits or changing fore- and hindlimb in different directions. We expect a similar pattern of high limb integration for *A. scriptus* populations (i.e., high positive correlations between fore- and hindlimbs), and that toepad area will be mostly correlated with the length of the corresponding longest finger or toe on which it was measured. Moreover, given that hurricane-induced selection resulted in an increase in the lengths of forelimb traits, but a reduction in the lengths of hindlimb traits (Donihue et al., 2018), we expect the evolutionary response to selection in the offspring to have not followed the direction of selection because fore- and hindlimbs are genetically correlated in anoles (McGlothlin et al., 2018, 2021). Yet, we also expect to see an increase in evolvability in the offspring if hurricane-induced selection reduced correlations between the limbs (i.e., if selection reduced the overall integration of limb traits due to the opposing direction of selection on fore- and hindlimbs).

2 | METHODS

2.1 | Sampling and morphological measurements

Anolis scriptus populations were sampled on two small islands in the Turks and Caicos: Pine Cay and Water Cay (350 and 250 ha, respectively). The islands are presently connected by a sandbar that was deposited by hurricane storm surge in the mid-1990s. However, the two populations are genetically distinct (unpublished data), and therefore can be treated as replicates of the response to extreme climatic events. Both cays are similarly covered by low vegetation (1 to 3 m in height). We sampled the anole populations along a 2-km transect on each island. The initial survey began on 28 August 2017 and lasted until 4 September 2017. We did not permanently mark individuals on the islands, and consequently, direct measures of individual survival are impossible. Hurricane Irma hit the Turks and Caicos on 8 September 2017 and Hurricane Maria passed through the region on 22 September 2017. Populations were revisited after the hurricanes between 16 October and 20 October 2017 and again approximately 18 months after the storms between 1 April 2019 and 8 April 2019. We caught 71 adult lizards in the initial survey, 93 during the 2017 revisit, and 117 lizards in 2019. This difference in sample size before and after the hurricane reflects an increased sampling effort after the hurricane. However, we do not expect these differences in sampling to strongly affect selection differentials and response to selection because these metrics are calculated using sample means of surveyed populations, and means are generally well estimated with just a few individuals (although standard errors are generally higher with smaller sample sizes).

To identify the most likely offspring of hurricane survivors in 2019, we calculated the maximum body size of a lizard that had hatched on 1 April 2018, one year before our revisit (following Donihue et al., 2020). To do this, we used a logistic-by-length model and estimated growth rates in ecologically similar species to characterize the growth curve of lizards (see Donihue et al., 2020 for details). By excluding lizards larger than this size threshold, we conservatively estimated the subset of the sampled population less than a year old and thus, offspring of hurricane survivors. We retained for further analyses only the sexually mature adults of each sampling period (i.e., pre-hurricane/post-hurricane/offspring) by using an adult body size threshold for each sex. See Supporting Information and Methods for a full description of the body size thresholds used. Our final sample sizes for each population were 36, 53 and 57 for Pine Cay, and 39, 52 and 57 for Water Cay, for pre-hurricane, post-hurricane, and offspring surveys, respectively.

All morphological measurements were taken by the same researcher on all three visits. Measurements included the snout-vent length (SVL), eight limb length segments, and toepad area on the fore- and hindlimbs (as described in Herrel et al., 2008; see also Lowie et al., 2019). For further details on the morphological measurements, see Supporting Information.

2.2 | Selection analysis and response to selection

To measure total hurricane-induced selection (indirect plus direct selection), we estimated a proxy of selection differentials (S), the mean trait difference between post- and pre-hurricane sampling periods (S = [mean traits of post] − [mean traits of pre]), which represent the survivors after selection and the population before selection, respectively. The selection differential should be a difference between the mean of parents of the next generation, after the hurricane, and the mean of pre-hurricane populations, thus we are assuming that most survivors reproduced. We calculated separate selection differentials for each island, given that the populations are genetically distinct, and they differed in mean trait values in the pre-hurricane survey (Table S1). To measure only the direct selection of traits, we estimated the corresponding selection gradients (β) for each island. We used two different equations: $\beta = P^{-1}S$ and $\beta = P^{-1}z$ (Lande & Arnold, 1983), where P^{-1} is the inverse of the phenotypic covariance matrix of limb traits in pre-hurricane populations and Δz is the response to selection. The second equation estimates β as the realized selection because it is based on the realized response to selection. We calculated the response to selection (Δz) for each island as the mean difference in traits between offspring and pre-hurricane populations. Inverting the P-matrix discounts the effects of trait correlations from the selection vector, retaining just direct selection on traits (Lande & Arnold, 1983). However, given that P-matrices are estimated with sampling error, their inversion makes more error accumulate in the smallest eigenvalues (which dominate the inverted P-matrix), biasing estimates of selection gradients. To correct for this bias, we performed a sampling noise control approach following Marroig et al. (2012), in which we replace the smallest unreliable eigenvalues of P-matrices with the last reliable eigenvalue (which is the sixth one for the *A. scriptus* P-matrices, determined using the second derivative of the distribution of eigenvalues). This procedure has been shown to improve the estimation of selection gradients (for more details, see Marroig et al., 2012). We explain below how we estimated P-matrices. Finally, we measured the vector correlation between both estimates of β to check if they are similar, and thus ensure that our assumption of post-hurricane population comprising mostly parents of the next generation holds true. To determine the significance of vector correlations, we randomly sampled 1000 vectors of 11 elements (number of traits) from a normal distribution of mean zero and unit SD and calculated their vector correlations. The critical values considering $\alpha = 0.05$ for this random distribution are −0.57 and 0.57. Therefore, any vector correlation below or above these values was considered significant.

To estimate uncertainty due to sampling error in our selection analysis, we performed bootstrapping of individuals caught on each survey on each island. We resampled with replacement 1000 times for each population and then we calculated the selection metrics on resampled populations, resulting in 1000 values of S and β. We extracted 95% confidence intervals (CI) for the selection metrics and if they did not encompass zero, the values were considered statistically significant. We also calculated 95% CI for mean-standardized selection to determine if the hurricane-induced selection is strong compared to the literature (Hereford et al., 2004) and for Δz values to determine if the offspring showed significant changes.

2.3 | P-matrices, overall integration and modularity of limb traits

We estimated P-matrices for each sampling period on each island to use as surrogates for G-matrices. Environmental effects leading to phenotypic plasticity may cause the P-matrix to differ from the G-matrix (Willis et al., 1991), but the potential for plasticity to impact traits in this study is likely low because growth after sexual maturity is limited. Moreover, Cheverud's conjecture has shown that well estimated G-matrices tend to resemble P-matrices (Cheverud, 1988), especially for morphological traits with generally high heritabilities (i.e., high contribution of genetic factors to overall variance), which is the case for lizard limb traits. Moreover, empirical examples of similarity between G and P are mounting in the literature (e.g., Marroig & Cheverud, 2001; Phillips & Arnold, 1999; Roff, 1996; Sodini et al., 2019; Styga et al., 2019). Finally, we compared *A. scriptus* P-matrices with a G-matrix of the closest relative, *A. cristatellus*, extracted from McGlothlin et al. (2018), and matrices are substantially similar (see Supporting Information, Tables S2 and S3). We also confirmed that P-matrices are reasonably well-estimated using a rarefaction analysis and we compared all P-matrices across populations of both islands (see Supporting Information and Figure S1). Given that $P = G + E$ (Falconer & Mackay, 1996), if P-matrices are similar, we may assume that P and G-matrices are also similar, otherwise the environmental matrix (E) in all populations would have to compensate for differences in G-matrices, which is a very unlikely scenario (Marroig & Cheverud, 2001). Even though it is preferable to use estimates of G-matrices to test the hypothesis of increased evolvability with strong selection induced by climatic extremes, because the potential to adapt ultimately depends on the heritable additive variation, estimating G-matrices in wild populations with appropriate sample sizes may be difficult. Despite this, the growing use of genomic data allowing the estimation of more precise G-matrices in a wide variety of organisms (Gienapp et al., 2017) will enable researchers to test this hypothesis more rigorously in the future.

To estimate the mean overall integration of traits in both Pine and Water Cays, we used correlation P-matrices and calculated an integration index using the variance of eigenvalues (egv), which is less prone to bias due to differences in sample size compared to other integration metrics if negligible eigenvalues are excluded (O'Keefe et al., 2022). This index is a ratio between the variance of eigenvalues and its theoretical maximum, which simply corresponds to the number of traits minus one (Pavlicev et al., 2009). To test if egv values differed between surveys, we used the 1000 bootstrapped populations to calculate 1000 P-matrices for each survey and extract a 95% CI of overall integration for each survey. If the 95% CI did not overlap between-surveys, we considered the differences in egv significant. We performed this analysis for all traits (including SVL), and separately for forelimbs and hindlimbs (excluding SVL) to check if one of the limbs showed a stronger response to hurricane-induced selection than the other.

We also performed a modularity analysis to explore the extent of integration of fore- and hindlimb components in relation to between-limb integration, and whether this pattern changed after the hurricanes. If the selection induced by the hurricane reduced the magnitude of between-limb correlations in the P-matrix, we expect to see an increase in limb modularity. We constructed three hypothetical modules: forelimb, hindlimb and toepad, the latter being composed of the toepad area of fore- and hindlimbs as well as the longest finger and longest toe. Even though toepads are epidermal modifications that likely develop from an embryonic origin semi-independent of the skeletal limb elements (Gamble, 2019; Liu et al., 2015; Weatherbee & Niswander, 2008), toepads are functionally linked to toes and fingers in locomotion (Elstrott & Irschick, 2004; Ruibal & Ernst, 1965), and therefore may constitute a functional module together with toes and fingers. We then tested whether average correlations within hypothetical modules (AVG+) were higher than between-modules (AVG−) using the empirical correlation P-matrices and a Mantel test to control for non-independence between correlations (Cheverud, 1995; Porto et al., 2013; using function 'TestModularity' in evolqg R package, Melo et al., 2015). Although the Mantel test is effective in detecting biologically meaningful modules when the modularity hypotheses are grounded in well-established developmental and functional studies as is our case here, we also tested modularity using a more recent test, the Covariance Ratio coefficient (CR), and permutations to calculate significance of effect sizes using the R package *geomorph* (Adams & Collyer, 2019; Adams & Otárola-Castillo, 2013). The CR is based on a ratio of within- and between-module covariances and gives standardized effect sizes (using Z-score transformations that take the scale-dependence of traits into account) that characterize the strength of the modular signal (Adams & Collyer, 2019).

2.4 | Evolvability analysis

Evolvability measures the amount of genetic variation in *G* in the direction of selection ($e(\beta) = (\beta^T G\beta)/|\beta|^2$, where ^{T} means transpose and $|\beta|^2$ is the squared strength of selection; Hansen & Houle, 2008). As we mentioned before, we substituted P-matrices for G-matrices to estimate evolvabilities. Thus, our interest was to compare evolvability in the directions of β before and after the hurricane to see if the P-matrices increased the amount of variation in the direction of selection, and to compare evolvability in the directions of β and *z*. If any of these vectors were aligned with trait correlations (i.e., aligned with pmax, the phenotypic equivalent of gmax), we expected their evolvability to be comparably high. To estimate the evolvability in the direction of selection, we then used the equation $e(\beta) = \beta^T P\beta$ (e.g., Assis et al., 2016; using function 'Evolvability' from evolqg R package, Melo et al., 2015) with β normalized to unit length and covariance P-matrices. Final $e(\beta)$ were standardized using the geometric mean of all traits to account for scale differences between traits and populations (e.g., Assis et al., 2016). We chose to standardize using a single value, the geometric mean of traits, instead of using the mean of each trait (e.g., Hansen & Houle, 2008) to preserve the structure of covariation.

We calculated two values of evolvability in the direction of selection for each island: (1) $e(\beta)$ before the hurricane: using pre-hurricane P-matrices and [post–pre] selection gradients, and (2) $e(\beta)$ after the hurricane: using offspring P-matrices and [post–pre] selection gradients. To estimate uncertainty in evolvability, we once again used the 1000 bootstrapped values of β and the 1000 bootstrapped P-matrices to construct 95% CI. This procedure accounts for errors in the estimation of both selection and P-matrices. We interpreted values as significantly different when 95% of the distributions did not overlap.

All analyses were conducted in the R programming environment (R Core Team, 2021, version 4.1). We provide the data and R scripts showing the selection and evolvability analyses, and showing the calculations to estimate inaccuracy in evolvability and the number of individuals needed to achieve a certain level of accuracy in Dryad and Zenodo.

3 | RESULTS

3.1 | Hurricane-induced direct selection on limb traits and response to selection

Selection (*S*) was mostly negative on traits, however, we only found significant negative selection on the hindlimb longest toe in Pine Cay (Table 1). In contrast, we found that several selection gradients (β) were significant on both island populations—mostly negative in SVL and hindlimb traits and positive for toepads. We also found positive direct selection on the humerus, but it was only significant on Water Cay (Table 1). Results were similar when using β vectors estimated with either *S* or *z*, given that both ways of calculating β resulted in significantly similar vectors (i.e., vector correlations of 0.86 for Pine Cay and 0.93 for Water Cay, both above the critical value of 0.57). Moreover, the selection was parallel in both islands, showing a vector correlation of 0.85. Interestingly, the mean-standardized β vectors are similar between-islands in magnitude, ranging from weak selection (around 0.05) to strong selection (around 0.7) when compared to the average mean-standardized β (0.89) found in Hereford et al. (2004) for morphological traits (see their Table 1). Response to selection (Δz) showed mostly a decrease in lengths of all traits, however, significant changes were only found in Pine Cay (Table 1). Δz vectors were not similar between populations, showing a nonsignificant vector correlation of 0.49. Whereas the response to selection was aligned with β in Water Cay (vector correlation of 0.84), this was not the case for Pine Cay (vector correlation of 0.48), even though both β vectors are not correlated with the axis of highest phenotypic variance (vector correlations of 0.0 and 0.05 with pmax, respectively). These results indicate that direct selection was parallel across islands, not aligned with the direction of most phenotypic variance, and the response in the offspring differed between the two islands.

3.2 | Pattern of limb trait correlations and overall integration

Correlation P-matrices are shown in Table S4. All correlation P-matrices show a PC1 that is predominantly isometric in size, with similar magnitudes of loadings for all traits and all loadings with the same sign (Table S5). Also, PC1 explains high amounts of proportional variation in all surveys, showing that variance accumulates in the direction of size. However, the pre-hurricane population in Water Cay shows less proportional variation accumulated in PC1 compared with Pine Cay. All P-matrices show a very high similarity when using Random Skewers (RS), with all values above 0.91, indicating that matrices respond similarly to random selection. Similarity of the best-matched PC axes (Krzanowski correlation, Krz) is in general lower, ranging from 0.70 to 0.79, which indicates that some PCs diverge across populations (Table 2). Still, P-matrices can be considered quite similar across populations, giving confidence in our assumption that *P* is a good surrogate of *G*.

We found a tendency for overall integration to be higher in post-hurricane populations, but the integration distributions overlap considerably (Figure 3a). The same pattern occurs if separating forelimb (95% CI for Pine Cay: pre = 0.21, 0.50; post = 0.36, 0.61; offspring = 0.19, 0.42; for Water Cay: pre = 0.12, 0.45; post = 0.25, 0.52; offspring = 0.18, 0.45; Figure 3b) and hindlimb (95% CI for Pine Cay: pre = 0.38, 0.73; post = 0.47, 0.73; offspring = 0.30, 0.60; for Water Cay: pre = 0.16, 0.5; post = 0.35, 0.65; offspring = 0.28, 0.60; Figure 3c). Results are the same if keeping all eigenvalues or just the

TABLE 1 Selection differentials (S), selection gradients (β), and response to selection (Δz) separated by island

	Traits	S (post–pre)	95% CI	β (post–pre)	95% CI	Δz (off–pre)	95% CI
Pine Cay							
Total size	SVL	−0.028	−0.088, 0.036	−0.187	**−0.269, −0.099**	−0.060	−0.124, 0.005
Hindlimb	Femur	−0.068	−0.133, 0.002	−0.179	**−0.253, −0.099**	−0.081	**−0.149, −0.010**
	Tibia	−0.033	−0.095, 0.034	−0.080	−0.160, 0.002	−0.054	−0.119, 0.0112
	Metatarsal	−0.033	−0.089, 0.028	0.003	−0.062, 0.071	−0.062	**−0.123, −0.002**
	Longest toe	−0.073	**−0.134, −0.008**	−0.303	**−0.413, −0.200**	−0.074	**−0.140, −0.008**
	Toepad area	0.057	−0.110, 0.230	0.186	**0.103, 0.265**	−0.068	−0.237, 0.100
Forelimb	Humerus	−0.017	−0.085, 0.057	0.062	−0.030, 0.161	−0.021	−0.087, 0.048
	Radius	−0.034	−0.093, 0.032	−0.095	**−0.160, −0.030**	−0.065	**−0.125, −0.007**
	Metacarp	−0.024	−0.080, 0.036	−0.048	−0.102, 0.008	0.012	−0.049, 0.071
	Longest finger	−0.040	−0.101, 0.030	−0.021	−0.085, 0.044	−0.040	−0.113, 0.031
	Toepad area	0.083	−0.075, 0.216	0.094	**0.035, 0.150**	−0.026	−0.195, 0.143
Water Cay							
Total size	SVL	−0.010	−0.065, 0.047	−0.101	**−0.146, −0.053**	−0.028	−0.085, 0.030
Hindlimb	Femur	−0.067	−0.137, 0.004	−0.290	**−0.394, −0.187**	−0.064	−0.130, 0.006
	Tibia	−0.009	−0.068, 0.051	−0.051	−0.129, 0.025	−0.024	−0.087, 0.037
	Metatarsal	0.000	−0.055, 0.059	−0.014	−0.067, 0.042	−0.035	−0.094, 0.022
	Longest toe	−0.030	−0.089, 0.033	−0.172	**−0.247, −0.101**	−0.023	−0.085, 0.040
	Toepad area	0.086	−0.074, 0.248	0.069	**0.010, 0.129**	0.046	−0.120, 0.218
Forelimb	Humerus	0.034	−0.028, 0.100	0.132	**0.067, 0.200**	0.009	−0.057, 0.075,
	Radius	−0.005	−0.061, 0.054	−0.045	−0.090, 0.005	−0.026	−0.087, 0.034
	Metacarp	0.031	−0.025, 0.093	−0.004	−0.065, 0.060	−0.003	−0.067, 0.062
	Longest finger	0.021	−0.050, 0.091	0.023	−0.055, 0.099	−0.011	−0.079, 0.058
	Toepad area	0.098	−0.061, 0.256	0.119	**0.050, 0.182**	0.038	−0.123, 0.205

Note: We show empirical values and the bootstrapped 95% CI. CI in bold are significant.

TABLE 2 Matrix similarity between all P-matrices

Matrix similarity		
Pine Cay	RS	Krz
Pre × post	0.96	0.76
Pre × offspring	0.95	0.73
Post × offspring	0.94	0.74
Water Cay	RS	Krz
Pre × post	0.92	0.71
Pre × offspring	0.92	0.79
Post × offspring	0.96	0.75
Pine Cay × Water Cay	RS	Krz
Pre	0.91	0.7
Post	0.97	0.74
Offspring	0.94	0.79

Note: We used two methods to compare P-matrices. Random skewers (RS) indicates the similarity in the response to random selection, whereas Krzanowski correlation (Krz) indicates similarity based on the best matched pairs of eigenvectors. All values are significant at $\alpha = 0.05$.

first six eigenvalues. Therefore, mean limb trait integration did not change with the hurricane-induced selection.

3.3 | Modularity of limb traits

The hindlimb is the only hypothetical module that shows higher average correlations within-module than between-modules, especially for Pine Cay populations (Figure 4). However, the hindlimb showed a signal of modularity that is significant only at $p = 0.10$ (Table S6). Therefore, forelimb, hindlimb and toepad traits can be seen as a single integrated unit. Still, we noticed that between-limb integration in pre-hurricane population was lower in Water Cay than in Pine Cay for both limbs (Figure 4b,c).

When using the CR coefficient, we found that both pre-hurricane populations have a significant CR coefficient. However, CR values are above 1.0 indicating that covariances within-modules are lower than between-modules. Moreover, we found no differences in pairwise comparisons of CR effect sizes across populations (Table S7, Figure S2). Therefore, we confirmed our results from the Mantel test

(a) Total Integration

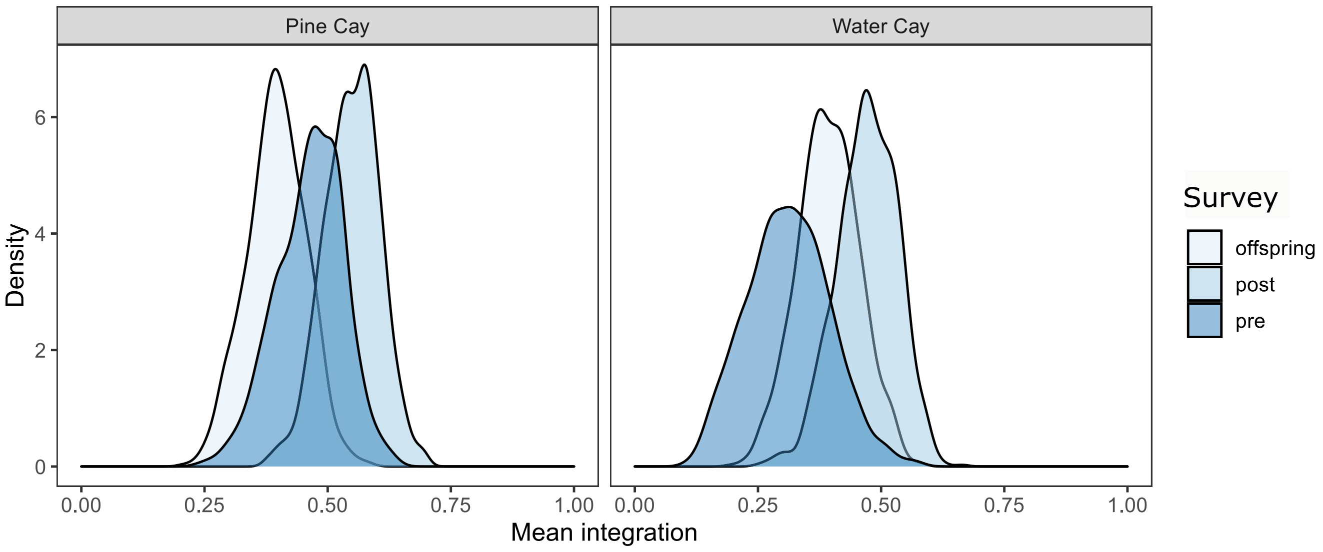

(b) Forelimb Integration

(c) Hindlimb Integration

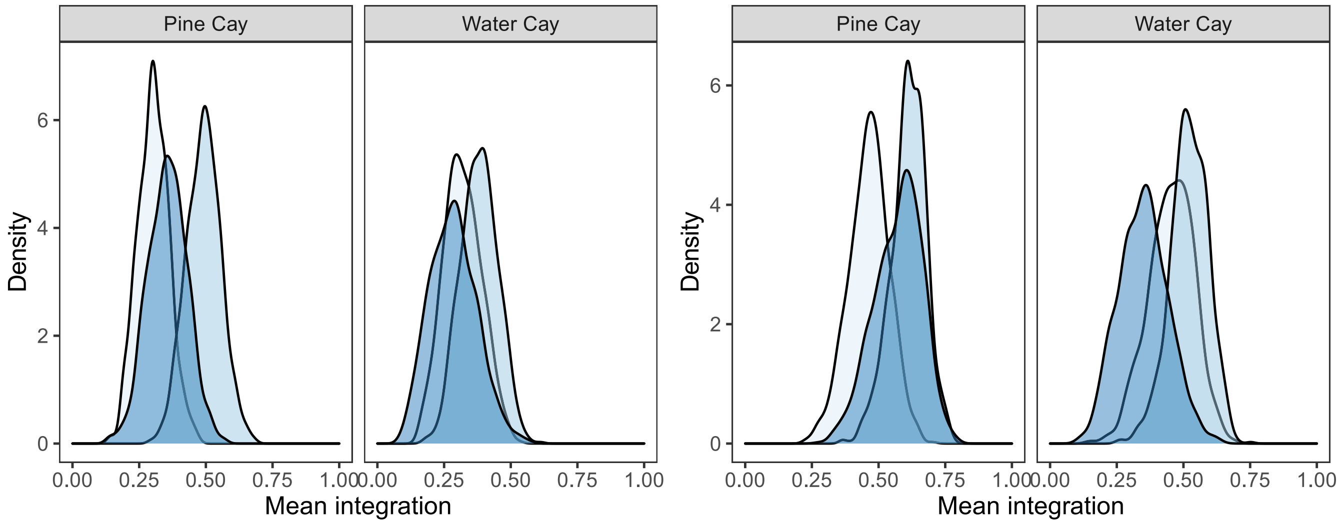

FIGURE 3 Mean overall integration of limb traits and toepad area. The values are eigenvalue variance of correlation P-matrices. (a) all traits. (b) Forelimb traits. (c) Hindlimb traits. The distributions were constructed by bootstrap resampling with 1000 iterations.

that the limbs are a single integrated unit in all populations and that the pattern did not change after the hurricane.

3.4 | Evolvability

We found a similar trend of increased evolvability in the direction of β from pre-hurricane parents to offspring in both islands (Table 3). However, the simulated confidence intervals are quite large, making these differences non-significant. This lack of significance may be due to low sample size to detect an evolvability difference. To determine the level of accuracy in our evolvability values, we used the analytical framework developed by Grabowski and Porto (2017), in which we could calculate the inaccuracy of evolvability given our sample size (lowest in pre-hurricane populations, around 35 individuals) and the overall integration of P-matrices (from 0.5 to 0.6). By looking at Figure S3a, our inaccuracy in evolvability ranged from 0.05 to 0.06. We also determined how many individuals we would need to find a significant difference (accuracy of 0.03 or lower) given the overall integration of P-matrices: we would need at least 65 to 75 individuals (Figure S3b).

4 | DISCUSSION

Incorporating multivariate adaptive responses of populations to climate change is a necessary step to better predict how and which species may overcome these challenges (Peschel et al., 2021). However, if climate-induced selection acts on multiple traits

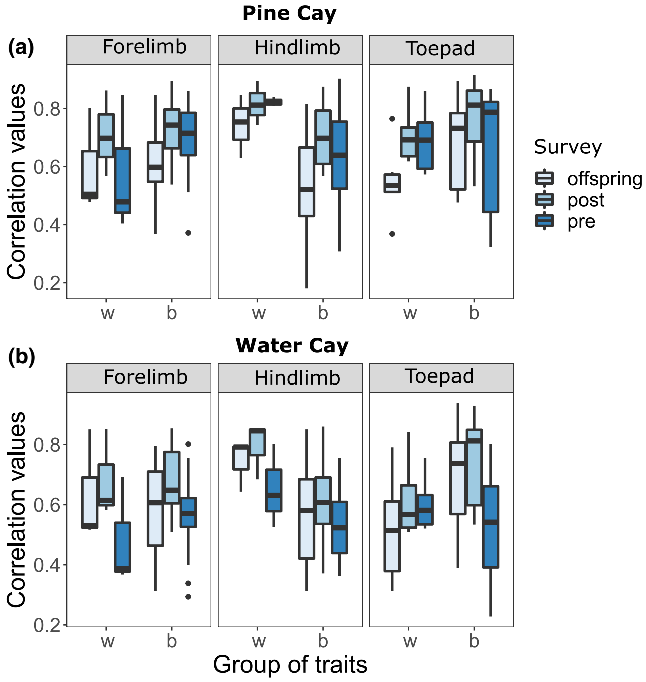

FIGURE 4 Average correlations within (w) and between (b) the three hypothetical modules. (a) Pine cay. (b) Water cay. Boxplots are showing the average correlation as a horizontal line. A set of traits is considered a module when within-set average correlation is higher than between-set average correlation. See Table S2 for the results of the modularity tests.

TABLE 3 Empirical evolvabilities and associated 95% confidence intervals

Evolvabilities	Pre $e(\beta)$	Offspring $e(\beta)$
Pine Cay	0.15	0.20
95% CI (simulations)	0.11, 0.19	0.14, 0.25
Water Cay	0.11	0.19
95% CI (simulations)	0.08, 0.22	0.14, 0.39

simultaneously and if traits are highly integrated, the response to selection may be constrained, not closely following the direction of selection (Chevin, 2012; Etterson & Shaw, 2001; Hellmann & Pineda-Krch, 2007). In this scenario, populations may not be able to cope with climate change even when responding to selection because the response would lead to a lower increase in mean fitness given that some traits will respond non-adaptively. This is especially likely if genetic correlations between positively selected traits are negative (e.g., Etterson & Shaw, 2001), but also if the selection is not aligned with axes accumulating the most variance in the G-matrix (Arnold et al., 2001; Walsh & Blows, 2009). Yet, if selection also changes the pattern of trait integration and increases the amount of genetic variance aligned with selection, future response to this same selection may be facilitated (Pavlicev et al., 2011). These alternative scenarios ultimately depend on the extent to which trait integration results in only a few directions accumulating most of the genetic variance, and how much selection is aligned with these directions (showing high evolvability; scenario B in Figure 1) or whether selection changes trait integration to increase evolvability.

We investigated these possibilities in a case study of an extreme climatic event, hurricane-induced selection on lizard limb traits (Donihue et al., 2018, 2020), in which we had samples of survivors and their offspring for two different populations. Given that selection was inferred to be strong on some of the limb traits (Donihue et al., 2018), we hypothesized that selection would change the pattern of limb integration and re-distribute genetic variation in a way that would increase the chance of adaptation to hurricanes in the future. Because we could not estimate G-matrices for the populations, our results are only suggestive but indicate that both populations had higher evolvability in the direction of selection after the hurricane, although this result was not significant. This lack of significance may be more related to a low sample size than to a genuinely non-significant effect, as we calculated that a sample size of around 70 individuals with the same evolvability values would lead to enough accuracy to find a significant difference in evolvability before and after the hurricane. Interestingly, our results raise the possibility that evolvability may increase after a single episode of selection and even if the direction of selection is not aligned with size (or PC1, the direction accumulates most genetic variance). Still, using P-matrices as surrogates of G-matrices likely may have overestimated evolvability values if environmental variation contributes to the total variation in the direction of selection. Alternatively, environmental variation may be much higher along pmax than gmax given that this direction is related to size, and several environmental factors can affect growth. In this case, evolvabilities can be underestimated by using P-matrices instead of G-matrices.

The model of directional selection influencing evolvability predicts changes in the pattern of correlation even with fluctuating selection, but the change depends on the level of epistasis between rQTLs and other genes (Pavlicev et al., 2011). Hence, it may be that only sustained or frequent directional selection, such as maintaining the same direction for several generations, would be able to increase evolvability in the direction of selection. Although we do not expect hurricane-induced selection to be this persistent because of its infrequency, lizard populations experiencing periodic hurricanes (up to four hurricanes over a 70-year period) show larger toepads than populations exposed to fewer hurricanes (Donihue et al., 2020), indicating that hurricanes can leave persistent marks on phenotypes. Moreover, hurricane frequency and magnitude are predicted to increase in the future due to climate change (Bender et al., 2010; Knutson et al., 2010).

4.1 | Direction of selection, locomotor performance and variation in responses to selection

Direct selection on limb traits in Pine Cay and Water Cay populations was parallel, giving some confidence in their estimation with the sampling noise control approach when inverting P-matrices

(Marroig et al., 2012). The parallel selection was also found in other lizard systems inferred to have suffered hurricane-induced selection (e.g., Rabe et al., 2020). The direct selection was strong in several limb traits, but not so strong on toepad area, although selection gradients were toward an increased surface area, and this is likely related to increased clinging capacity in *A. scriptus* (Crandell et al., 2014; Donihue et al., 2018). However, shifts in toepad area do not always lead to higher clinging capacity in lizards (e.g., Dufour et al., 2019) and other traits beyond toepad area also change clinging capacity (such as setae length and limb length; Hagey et al., 2014; Kolbe, 2015). Direct selection to reduce femur length was stronger, supporting the evidence in favour of reduced aerodynamic drag in lizards that have smaller hindlimbs and consequently exposing less of the pelvic region to the strong winds induced by hurricanes (Debaere et al., 2021). Thus, selection induced by hurricanes, and possibly selection induced by other climatic events, may vary in direction and strength on different traits, showing the relevance of using a multivariate approach to estimate selection.

Another source of variation induced by climatic events is how much the responses are constrained by trait integration. Fore- and hindlimbs compose a single integrated unit in both populations. This high between-limb integration was expected from previous studies (Kolbe et al., 2011; McGlothlin et al., 2018) and likely results from the need to coordinate both limbs in locomotion (Aerts et al., 2000). However, populations may still differ in the strength of between-limb integration. For instance, the modularity analysis showed that between-limb correlations were lower in Water Cay than in Pine Cay, and the former had a morphological response that followed much more closely the direction of selection than Pine Cay (vector correlation of 0.84 compared with 0.48, respectively). Because direct selection was not aligned with limb integration in either of the populations (i.e., selection did not increase or decrease all limb traits, as evidenced by the lower correlation between β and pmax), the lower correlations between limbs may have resulted in less correlated responses of limb elements in Water Cay, and therefore, a lower constraint in the direction of the response to selection. Finally, we must also consider that populations may differ due to chance and evolutionary forces unrelated to selection, and having more than two populations in future studies will aid in evaluating the consistency of patterns of selection and responses to selection induced by hurricanes.

Therefore, although extreme climatic events like hurricanes are predicted to become more frequent and intense with future climate change (Bender et al., 2010; Knutson et al., 2010), the responses of lizard populations may vary because of differences in strength of selection, and differences in trait integration resulting in different degrees of constrained responses to selection. A broader implication of all these sources of variation for responses to climate-driven selective pressures is the resultant variation in how long these changes last in terms of evolutionary time. For traits experiencing stronger selection and having lower genetic correlations, a longer-lasting evolutionary response to extreme climatic events may be more common, as shown for populations and species more often hit by hurricanes showing larger toepads (Donihue et al., 2020). On the other hand, for traits that show a more constrained response because of high trait integration, the evolutionary responses may be more ephemeral.

4.2 | Selection of trait integration patterns and evolvability

Even though we found evidence for strong selection on some limb traits in both populations, integration patterns were not changed by this selection, suggesting that only very strong selection (or lesser magnitude of selection sustained over multiple generations) can redistribute variation in the G-matrix. For instance, in two different species of chipmunks that experienced selection induced by 100 years of climate change, only the species under stronger selection showed increased evolvability after selection (Assis et al., 2016). Whether strong selection changes trait integration, and perhaps also evolvability, may be related to a conflict with multivariate stabilizing selection (Cheverud, 1984; Roff & Fairbairn, 2012) associated with the maintenance of a pattern of higher correlations among traits that perform the same function. In this scenario, the G-matrix is kept evolutionarily conserved by a stable pattern of correlational selection, that in the case of lizard limbs would be associated with locomotor tasks normally performed in the environment (e.g., sprinting, jumping, climbing; Foster & Higham, 2012; Irschick & Losos, 1998; Perry et al., 2004). These performances demand a coordination between the fore- and hindlimbs, and thus selection to enhance these performances would favour high integration between limbs (McGlothlin et al., 2018). This conflict between episodes of directional selection causing short-term, fast changes in *G*, and multivariate stabilizing selection promoting long-term evolutionary stability in *G*, must be common in nature given that different types of selection may act on populations (Arnold et al., 2008). Selective forces and other factors, such as mutation, all influence simultaneously the G-matrix and the balance between these factors ultimately shape the evolutionary potential of populations. Therefore, hurricane-induced selection on *A. scriptus* limbs in the Turks and Caicos appears to conflict with a selection associated with normal environmental conditions with the latter being much more persistent. Hence, the P- and G-matrices of *A. scriptus* are likely shaped by multivariate selection related to normal limb functioning to a much greater extent than by hurricane-induced selection, even if these extreme selection events are much stronger than selection in normal ecological conditions. Even for populations subjected to hurricanes in a higher frequency, selection in normal ecological conditions may erase any potential long-lasting signal of lower limb integration due to hurricane-induced selection.

5 | CONCLUSION

We showed how the hypothesis of directional selection leading to increased evolvability can be studied in the context of population-wide responses to extreme climatic events. Ideally, this hypothesis should be tested with G-matrices with appropriate sample sizes before and after the extreme event, which is likely above 70 individuals if studying around 10 traits. Although we expected strong hurricane-induced selection to reduce limb trait integration, this did not happen in *A. scriptus* populations, potentially because the episodic selection caused by this hurricane was not persistent enough to contrast normal ecological conditions, despite hurricanes being a relatively strong selective force. Even so, our results indicate that evolutionary responses follow more closely the direction of selection more if between-limb integration is lower. Therefore, the persistence of populations facing strong environmental changes may be enhanced by lower trait integration, even if individuals perform normal functions at a lower level than more highly integrated individuals in normal ecological conditions.

AUTHOR CONTRIBUTIONS

Monique Nouailhetas Simon: Conceptualization (supporting); formal analysis (lead); methodology (equal); visualization (lead); writing – original draft (lead). **Priscila Rothier:** Conceptualization (supporting); formal analysis (supporting); methodology (equal); writing – review and editing (supporting). **Colin Donihue:** Conceptualization (lead); formal analysis (supporting); investigation (lead); resources (lead); writing – review and editing (equal). **Anthony Herrel:** Conceptualization (lead); funding acquisition (lead); investigation (lead); project administration (equal); resources (lead); supervision (equal); writing – review and editing (equal). **Jason J. Kolbe:** Conceptualization (lead); funding acquisition (lead); investigation (equal); methodology (equal); project administration (equal); resources (lead); supervision (lead); writing – review and editing (lead).

ACKNOWLEDGEMENTS

This work was made possible thanks to the Pine Cay Homeowners Association and the US National Science Foundation. All the procedures were approved by the Turks and Caicos DECR (Initial Permit: 17-08-02-14; Revisit Permit: 17-10-01-15) and Harvard University IACUC (26-11). We thank C. Santoro and A-C. Fabre for help in the field. A-C. Fabre came up with the initial idea for the study. We also thank Jonathan Losos, Adam Siepielski and Gabriel Marroig for their comments and suggestions on a previous version.

CONFLICT OF INTEREST

The authors declare no conflicts of interest.

PEER REVIEW

The peer review history for this article is available at https://publons.com/publon/10.1111/jeb.14115.

DATA AVAILABILITY STATEMENT

Raw data is deposited in Dryad; Simon, Monique et al. (2022), Data from: Can extreme climatic events induce shifts in adaptive potential? Dryad, Dataset, https://doi.org/10.5061/dryad.05qfttf3w. Code for analysis is deposited in Zenodo, https://zenodo.org/record/6965042#.Y2BORXbMKUk

ORCID

Monique N. Simon https://orcid.org/0000-0003-0106-2660
Priscila S. Rothier https://orcid.org/0000-0003-3017-6528
Colin M. Donihue https://orcid.org/0000-0003-1096-8536
Anthony Herrel https://orcid.org/0000-0003-0991-4434

REFERENCES

Adams, D. C., & Collyer, M. L. (2019). Comparing the strength of modular signal, and evaluating alternative modular hypotheses, using covariance ratio effect sizes with morphometric data. *Evolution*, *73*, 2352–2367.

Adams, D. C., & Otárola-Castillo, E. (2013). Geomorph: An R package for the collection and analysis of geometric morphometric shape data. *Methods in Ecology and Evolution*, *4*, 393–399.

Aerts, P., Van Damme, R., Vanhooydonck, B., Zaaf, A., & Herrel, A. (2000). Lizard locomotion: How morphology meets ecology. *Netherlands Journal of Zoology*, *50*, 261–278.

Arnold, S. J., Bürger, R., Hohenlohe, P. A., Ajie, B. C., & Jones, A. G. (2008). Understanding the evolution and stability of the G-matrix. *Evolution*, *62*, 2451–2461.

Arnold, S. J., Pfrender, M. E., & Jones, A. G. (2001). The adaptive landscape as a conceptual bridge between micro- and macroevolution. In A. P. Hendry & M. T. Kinnison (Eds.), *Microevolution rate, pattern, process* (pp. 9–32). Springer-Science + Business Media, B.V.

Assis, A. P. A., Patton, J. L., Hubbe, A., & Marroig, G. (2016). Directional selection effects on patterns of phenotypic (co)variation in wild populations. *Proceedings of the Royal Society B: Biological Sciences*, *283*, 20161615.

Bender, M. A., Knutson, T. R., Tuleya, R. E., Sirutis, J. J., Vecchi, G. A., Garner, S. T., & Held, I. M. (2010). Modeled impact of anthropogenic warming on the frequency of intense Atlantic hurricanes. *Science*, *327*, 454–458.

Burger, R. (1993). Prediction of the dynamics of a polygenic character under directional selection. *Journal of Theoretical Biology*, *162*, 487–513.

Calsbeek, R., & Bonneaud, C. (2008). Postcopulatory fertilization bias as a form of cryptic sexual selection. *Evolution*, *62*, 1137–1148.

Cheverud, J. M. (1984). Quantitative genetics and developmental constraints on evolution by selection. *Journal of Theoretical Biology*, *110*, 155–171.

Cheverud, J. M. (1988). A comparison of genetic and phenotypic correlations. *Evolution*, *42*, 958–968.

Cheverud, J. M. (1995). Morphological integration in the saddle-Back tamarin (*Saguinus fuscicollis*) cranium. *The American Naturalist*, *145*, 63–89.

Cheverud, J. M., Ehrich, T. H., Vaughn, T. T., Koreishi, S. F., Linsey, R. B., & Pletscher, L. S. (2004). Pleiotropic effects on mandibular morphology II: Differential epistasis and genetic variation in morphological integration. *The Journal of Experimental Zoology*, *302B*, 424–435.

Chevin, L.-M. (2012). Genetic constraints on adaptation to a changing environment. *Evolution*, *67*, 708–721.

Crandell, K. E., Herrel, A., Sasa, M., Losos, J. B., & Autumn, K. (2014). Stick or grip? Co-evolution of adhesive toepads and claws in *Anolis* lizards. *Zoology*, *117*, 363–369.

Debaere, S. F., Donihue, C. M., Herrel, A., & Van Wassenbergh, S. (2021). An aerodynamic perspective on hurricane-induced selection on *Anolis* lizards. *Functional Ecology*, *35*(9), 2026–2032.

Diniz-Filho, J. A. F., Souza, K. S., Bini, L. M., Loyola, R., Dobrovolski, R., Rodrigues, J. F. M., de Lima-Ribeiro, M. S., Terribile, L. C., Rangel, T. F., Bione, I., & Freitas, R. (2019). A macroecological approach to evolutionary rescue and adaptation to climate change. *Ecography*, *42*, 1124–1141.

Donihue, C. M., Herrel, A., Fabre, A.-C., Kamath, A., Geneva, A. J., Schoener, T. W., Kolbe, J. J., & Losos, J. B. (2018). Hurricane-induced selection on the morphology of an Island lizard. *Nature*, *560*, 88–91.

Donihue, C. M., Kowaleski, A. M., Losos, J. B., Algar, A. C., Baeckens, S., Buchkowski, R. W., Fabre, A.-C., Frank, H. K., Geneva, A. J., Reynolds, R. G., Stroud, J. T., Velasco, J. A., Kolbe, J. J., Mahler, D. L., & Herrel, A. (2020). Hurricane effects on neotropical lizards span geographic and phylogenetic scales. *Proceedings of the National Academy of Sciences of the United States of America*, *117*, 10429–10434.

Dufour, C. M. S., Donihue, C. M., Losos, J. B., & Herrel, A. (2019). Parallel increases in grip strength in two species of *Anolis* lizards after a major hurricane on Dominica. *Journal of Zoology*, *309*, 77–83.

Elstrott, J., & Irschick, D. J. (2004). Evolutionary correlations among morphology, habitat use and clinging performance in Caribbean *Anolis* lizards. *Biological Journal of the Linnean Society*, *83*, 389–398.

Etterson, J. R. (2004). Evolutionary potential of *Chamaecrista fasciculata* in relation to climate change. II. Genetic architecture of three populations reciprocally planted along an environmental gradient in the great plains. *Evolution*, *58*, 1459–1471.

Etterson, J. R., & Shaw, R. G. (2001). Constraint to adaptive evolution in response to global warming. *Science*, *294*, 151–154.

Falconer, D. S., & Mackay, T. (1996). *Introduction to quantitative genetics* (4th ed.). Addison Wesley Longman.

Fischer, E. M., Sippel, S., & Knutti, R. (2021). Increasing probability of record-shattering climate extremes. *Nature Climate Change*, *11*, 689–695.

Foster, K. L., & Higham, T. E. (2012). How forelimb and hindlimb function changes with incline and perch diameter in the green anole, *Anolis carolinensis*. *Journal of Experimental Biology*, *215*, 2288–2300.

Gamble, T. (2019). Duplications in corneous Beta protein genes and the evolution of gecko adhesion. *Integrative and Comparative Biology*, *59*, 193–202.

Gienapp, P., Fior, S., Guillaume, F., Lasky, J. R., Sork, V. L., & Csilléry, K. (2017). Genomic quantitative genetics to study evolution in the wild. *Trends in Ecology & Evolution*, *32*, 897–908.

Grabowski, M., & Porto, A. (2017). How many more? Sample size determination in studies of morphological integration and evolvability. *Methods in Ecology and Evolution*, *8*, 592–603.

Grant, P. R., Grant, B. R., Huey, R. B., Johnson, M. T. J., Knoll, A. H., & Schmitt, J. (2017). Evolution caused by extreme events. *Philosophical Transactions of the Royal Society B: Biological Sciences*, *372*, 20160146.

Hagey, T. J., Puthoff, J. B., Holbrook, M., Harmon, L. J., & Autumn, K. (2014). Variation in setal micromechanics and performance of two gecko species. *Zoomorphology*, *133*, 111–126.

Hansen, T. F., & Houle, D. (2008). Measuring and comparing evolvability and constraint in multivariate characters. *Journal of Evolutionary Biology*, *21*, 1201–1219.

Hellmann, J. J., & Pineda-Krch, M. (2007). Constraints and reinforcement on adaptation under climate change: Selection of genetically correlated traits. *Biological Conservation*, *137*, 599–609.

Hereford, J., Hansen, T. F., & Houle, D. (2004). Comparing strengths of directional selection: How strong is strong? *Evolution*, *58*, 2133–2143.

Herrel, A., Huyghe, K., Vanhooydonck, B., Backeljau, T., Breugelmans, K., Grbac, I., Van Damme, R., & Irschick, D. J. (2008). Rapid large-scale evolutionary divergence in morphology and performance associated with exploitation of a different dietary resource. *Proceedings of the National Academy of Sciences of the United States of America*, *105*, 4792–4795.

Hill, W. G. (1982). Rates of change in quantitative traits from fixation of new mutations. *Proceedings of the National Academy of Sciences of the United States of America*, *79*, 142–145.

Houle, D. (1992). Comparing evolvability and variability of quantitative traits. *Genetics*, *130*, 195–204.

Irschick, D. J., & Losos, J. B. (1998). A comparative analysis of the ecological significance of maximal locomotor performance in Caribbean *Anolis* lizards. *Evolution*, *52*, 219–226.

Jones, A. G., Bürger, R., & Arnold, S. J. (2014). Epistasis and natural selection shape the mutational architecture of complex traits. *Nature Communications*, *5*, 3709.

Knutson, T. R., McBride, J. L., Chan, J., Emanuel, K., Holland, G., Landsea, C., Held, I., Kossin, J. P., Srivastava, A. K., & Sugi, M. (2010). Tropical cyclones and climate change. *Nature Geoscience*, *3*, 157–163.

Kolbe, J. J. (2015). Effects of hind-limb length and perch diameter on clinging performance in *Anolis* lizards from the British Virgin Islands. *Journal of Herpetology*, *49*, 284–290.

Kolbe, J. J., Revell, L. J., Szekely, B., Brodie, E. D., III, & Losos, J. B. (2011). Convergent evolution of phenotypic integration and its alignment with morphological diversification in Caribbean *Anolis* ecomoprhs. *Evolution*, *65*, 3608–3624.

Lande, R. (1979). Quantitative genetic analysis of multivariate evolution, applied to brain: Body size allometry. *Evolution*, *33*, 402–416.

Lande, R., & Arnold, S. J. (1983). The measurement of selection on correlated characters. *Evolution*, *37*, 1210–1236.

Liu, Y., Zhou, Q., Wang, Y., Luo, L., Yang, J., Yang, L., Liu, M., Li, Y., Qian, T., Zheng, Y., Li, M., Li, J., Gu, Y., Han, Z., Xu, M., Wang, Y., Zhu, C., Yu, B., Yang, Y., … Gu, X. (2015). Gekko japonicus genome reveals evolution of adhesive toe pads and tail regeneration. *Nature Communications*, *6*, 10033.

Lowie, A., Gillet, E., Vanhooydonck, B., Irschick, D. J., Losos, J. B., & Herrel, A. (2019). Do the relationships between hind limb anatomy and sprint speed variation differ between sexes in *Anolis* lizards? *Journal of Experimental Biology*, *222*(5), jeb.188805.

Marroig, G., & Cheverud, J. M. (2001). A comparison of phenotypic variation and covariation patterns and the role of phylogeny, ecology, and ontogeny during cranial evolution of new world monkeys. *Evolution*, *55*, 2576–2600.

Marroig, G., Melo, D. A., & Garcia, G. (2012). Modularity, noise, and natural selection. *Evolution*, *66*, 1506–1524.

McGlothlin, J. W., Kobiela, M. E., Wright, H. V., & Kolbe, J. J. (2021). The adaptive radiation of *Anolis* lizards. *bioRxiv*, *46*.

McGlothlin, J. W., Kobiela, M. E., Wright, H. V., Mahler, D. L., Kolbe, J. J., Losos, J. B., & Brodie, E. D. (2018). Adaptive radiation along a deeply conserved genetic line of least resistance in *Anolis* lizards. *Evolution Letters*, *2*, 310–322.

Melo, D., Garcia, G., Hubbe, A., Assis, A. P., & Marroig, G. (2015). EvolQG: An R package for evolutionary quantitative genetics. *F1000Research*, *4*, 925.

Melo, D., & Marroig, G. (2015). Directional selection can drive the evolution of modularity in complex traits. *Proceedings of the National Academy of Sciences of the United States of America*, *112*, 470–475.

Nadeau, C. P., & Urban, M. C. (2019). Eco-evolution on the edge during climate change. *Ecography*, *42*, 1280–1297.

O'Keefe, F. R., Meachen, J. A., & Polly, P. D. (2022). On information rank deficiency in phenotypic covariance matrices. *Systematic Biology*, *71*, 810–822.

Pavlicev, M., Cheverud, J. M., & Wagner, G. P. (2009). Measuring morphological integration using eigenvalue variance. *Evolutionary Biology*, *36*, 157–170.

Pavlicev, M., Cheverud, J. M., & Wagner, G. P. (2011). Evolution of adaptive phenotypic variation patterns by direct selection for evolvability. *Proceedings of the Royal Society B: Biological Sciences*, *278*, 1903–1912.

Pavlicev, M., Kenney-Hunt, J. P., Norgard, E. A., Roseman, C. C., Wolf, J. B., & Cheverud, J. M. (2008). Genetic variation in pleiotropy: Differential epistasis as a source of variation in the allometric relationship between long bone lengths and body weight. *Evolution*, *62*, 199–213.

Penna, A., Melo, D., Bernardi, S., Oyarzabal, M. I., & Marroig, G. (2017). The evolution of phenotypic integration: How directional selection reshapes covariation in mice. *Evolution*, *71*, 2370–2380.

Perry, G., LeVering, K., Girard, I., & Garland, T. (2004). Locomotor performance and social dominance in male *Anolis cristatellus*. *Animal Behaviour*, *67*, 37–47.

Peschel, A. R., Boehm, E. L., & Shaw, R. G. (2021). Estimating the capacity of *Chamaecrista fasciculata* for adaptation to change in precipitation. *Evolution*, *75*, 73–85.

Phillips, P. C., & Arnold, S. J. (1999). Hierarchical comparison of genetic variance-covariance matrices. I. Using the flury hierarchy. *Evolution*, *53*, 1506–1515.

Porto, A., Shirai, L. T., de Oliveira, F. B., & Marroig, G. (2013). Size variation, growth strategies, and the evolution of modularity in the mammalian skull. *Evolution*, *67*, 3305–3322.

Quintero, I., & Wiens, J. J. (2013). What determines the climatic niche width of species? The role of spatial and temporal climatic variation in three vertebrate clades. *Global Ecology and Biogeography*, *22*, 422–432.

R Core Team. (2021). *R: A language and environment for statistical computing, version 4.1.0*. R Foundation for Statistical Computing. https://www.R-project.org/

Rabe, A. M., Herrmann, N. C., Culbertson, K. A., Donihue, C. M., & Prado-Irwin, S. R. (2020). Post-hurricane shifts in the morphology of Island lizards. *Biological Journal of the Linnean Society*, *130*, 156–165.

Roff, D. A. (1996). The evolution of genetic correlations: An analysis of patterns. *Evolution*, *50*, 1392–1403.

Roff, D. A., & Fairbairn, D. J. (2012). A test of the hypothesis that correlational selection generates genetic correlations. *Evolution*, *66*, 2953–2960.

Ruibal, R., & Ernst, V. (1965). The structure of the digital setae of lizards. *Journal of Morphology*, *117*, 271–293.

Sodini, S. M., Kemper, K. E., Wray, N. R., & Trzaskowski, M. (2019). Comparison of genotypic and phenotypic correlations: Cheverud's conjecture in humans. *Genetics*, *209*, 941–948.

Styga, J. M., Houslay, T. M., Wilson, A. J., & Earley, R. L. (2019). Development of G: A test in an amphibious fish. *Heredity*, *122*, 696–708.

Walsh, B., & Blows, M. W. (2009). Abundant genetic variation + strong selection = multivariate genetic constraints: A geometric view of adaptation. *Annual Review of Ecology, Evolution, and Systematics*, *40*, 41–59.

Weatherbee, S. D., & Niswander, L. A. (2008). *Chapter 7: Mechanisms of chondrogenesis and osteogenesis in limbs*. In B. K. Hall (Ed.), (pp. 93–102). University of Chicago Press.

Willis, J. H., Coyne, J. A., & Kirkpatrick, M. (1991). Can one predict the evolution of quantitative characters without genetics? *Evolution*, *45*, 441–444.

SUPPORTING INFORMATION

Additional supporting information can be found online in the Supporting Information section at the end of this article.

How to cite this article: Simon, M. N., Rothier, P. S., Donihue, C. M., Herrel, A., & Kolbe, J. J. (2022). Can extreme climatic events induce shifts in adaptive potential? A conceptual framework and empirical test with *Anolis* lizards. *Journal of Evolutionary Biology*, *00*, 1–14. https://doi.org/10.1111/jeb.14115